The British Journal of Radiology, 84 (2011), 833–842

Biodosimetric quantification of short-term synchrotron microbeam versus broad-beam radiation damage to mouse skin using a dermatopathological scoring system

[1,2]R C U PRIYADARSHIKA, MBBS, MD, [3,4,5,6]J C CROSBIE, MSc, PhD, [1]B KUMAR, MD, FRCPA and [3,6]P A W ROGERS, PhD

[1]*Department of Pathology, Southern Health, Monash Medical Centre, Clayton, Victoria, Australia,* [2]*Department of Pathology, Base Hospital, Kuliyapitiya, Sri Lanka,* [3]*Centre for Women's Health Research, Department of Obstetrics and Gynaecology and Monash Institute of Medical Research,* [4]*Monash Centre for Synchrotron Science, Monash University, Clayton,* [5]*The William Buckland Radiotherapy Centre, Alfred Hospital, Melbourne, and* [6]*Department of Obstetrics and Gynaecology, University of Melbourne, The Royal Women's Hospital, Flemington Road and Grattan Street, Parkville, Victoria, Australia*

Objectives: Microbeam radiotherapy (MRT) with wafers of microscopically narrow, synchrotron generated X-rays is being used for pre-clinical cancer trials in animal models. It has been shown that high dose MRT can be effective at destroying tumours in animal models, while causing unexpectedly little damage to normal tissue. The aim of this study was to use a dermatopathological scoring system to quantify and compare the acute biological response of normal mouse skin with microplanar and broad-beam (BB) radiation as a basis for biological dosimetry.
Method: The skin flaps of three groups of mice were irradiated with high entrance doses (200 Gy, 400 Gy and 800 Gy) of MRT and BB and low dose BB (11 Gy, 22 Gy and 44 Gy). The mice were culled at different time-points post-irradiation. Skin sections were evaluated histologically using the following parameters: epidermal cell death, nuclear enlargement, spongiosis, hair follicle damage and dermal inflammation. The fields of irradiation were identified by γH2AX-positive immunostaining.
Results: The acute radiation damage in skin from high dose MRT was significantly lower than from high dose BB and, importantly, similar to low dose BB.
Conclusion: The integrated MRT dose was more relevant than the peak or valley dose when comparing with BB fields. In MRT-treated skin, the apoptotic cells of epidermis and hair follicles were not confined to the microbeam paths.

Received 19 August 2010
Revised 31 January 2011
Accepted 1 February 2011

DOI: 10.1259/bjr/58503354

Synchrotron microbeam radiotherapy (MRT) uses wafers of microscopically narrow, synchrotron-generated X-rays for pre-clinical cancer trials in animal models [1–6]. Previous studies have shown normal tissue to be extremely tolerant to MRT at doses in considerable excess of those that were therapeutically effective [7]. Further, MRT has been proven to have palliative and even curative effects on cerebral tumours implanted in rat brains [1, 8]. The interpretation of the effects of MRT on biological tissue is complicated by difficulties in accurately measuring the absorbed dose deposited in tissue by MRT. Physical dosimetry associated with MRT is more complex than that for conventional broad-beam (BB) radiotherapy because there are different components to an MRT dose profile [9–12]. These components include the in-beam or "peak" dose, the valley dose (between adjacent microbeams) and the integrated dose. Dilmanian et al [13] defined the integrated dose as "the microbeam dose averaged over the entire irradiation area" and further "the integrated dose takes into account the volume of tissue in the low dose regions between the microbeams". Zhong et al [7] stated that the "integrated microbeam doses, (which for low valley doses) can be approximated as the in-beam dose times the ratio of the beam width to beam spacing". There exists a vast body of literature over several decades on the acute effects of radiation therapy on skin tissue (radiodermatitis), some of which have been documented in review articles [14, 15] and text books [16–19]. McKee et al [20] state:

> The histological features of acute radiation damage to skin involve both the epidermis and its adnexae, and the underlying dermis. The epithelium may be necrotic and accompanied by both spongiosis (inter-cellular oedema) and intra-cellular edema. The dermis is edematous and may show fibrin deposition. An inflammatory cell infiltrate consisting of macrophages, eosinophils, plasma cells and lymphocytes is present in the dermis.

Address correspondence to: Professor Peter Rogers, University of Melbourne Dept of Obstetrics & Gynaecology, The Royal Women's Hospital, Flemington Road and Grattan Street, Parkville, Victoria 3052, Australia. E-mail: parogers@unimelb.edu.au

Further, Lever and Schaumburg-Lever [21] state:

> The cells of the hair follicles, sebaceous glands, and sweat glands also show degenerative changes. Some of the blood vessels are dilated, whereas others, especially large ones in the deep portions of the dermis show edema of their walls, endothelium and even thrombosis. The collagen bundles show edema. In cases with blisters, the degenerated epidermis is detached from the dermis, and, if ulceration is present, not only the epidermis but also the upper dermis has undergone necrosis. The area of necrosis is then surrounded by neutrophils.

The effects of synchrotron MRT on skin are less well documented [7, 22] and to our knowledge a quantitative, histopathological comparison of MRT and BB has not been reported. The aim of this study was to use a histopathological skin scoring system to quantify the acute biological response of normal mouse skin to MRT and BB irradiations as a basis of biological dosimetry. We hypothesise high dose BB (hundreds of Gy) will cause more skin damage than high dose MRT for the same peak entrance dose. Further, low dose BB (tens of Gy) will cause equivalent levels of damage as high dose MRT.

Methods and materials

Synchrotron radiation source and microbeam generation

All irradiations were carried out on beamline BL28B2 (SPring-8 synchrotron, Hyogo, Japan). A bending magnet produces polychromatic X-rays from electrons travelling at relativistic speeds around a storage ring with energies of 8 GeV and a stable beam current of approximately 100 mA. The synchrotron X-ray beam was filtered by passing through a 3 mm-thick copper absorber that preferentially absorbs low energy X-rays and hence increases the beam's mean energy. The mean energy of the filtered X-ray beam was 125 keV [23]. A tungsten/kapton collimator segmented the BB into a lattice of planar microbeams. The thickness of the tungsten/kapton collimator in the direction of the beam was approximately 5 mm. The nominal beam width was 25 μm (industrial-grade kapton sheets). Ohno et al [23] reported the effective beam width for this collimator at full width half maximum was 21.2–23.1 μm with a centre-to-centre spacing of exactly 200 μm. The peak-to-valley dose ratio for this collimator was measured using radiochromic films of different sensitivity. In a solid water phantom, the dose in the valley region is typically between 1% and 2% of the dose in the peaks. A complete description of the dosimetry used for this MRT research is described elsewhere [10, 23].

Mouse preparation

Adult female mice (ddY and BALB/C strain) aged 11 weeks were used for this study. All experimental protocols were approved by the animal welfare committees of the Japanese Synchrotron Radiation Research Institute (SPring-8) and Monash University (MMCAECA). The animals were fed a standard rodent diet and given water *ad libitum* in the animal house of the biomedical imaging centre on the SPring-8 synchrotron campus. The animals were anaesthetised using a 1:10 dilution of pentobarbitone (Nembutal, Sigma Aldrich, St Louis, MO) at a concentration of approximately 1 ml kg^{-1} (equivalent to 50 mg kg^{-1} body weight). The hair along the animals, back was shaved using a standard electric rodent shaver. A skin flap was raised along the animals' back and pre-cut lengths of radiochromic film (Gafchromic HD-810, ISP Corp, Wayne, NJ) were placed on both sides of the skin flap to demarcate the entrance and exit radiation fields. The mice were secured on a perspex jig by placing them inside a 50 ml vial with a cut-away made to expose the raised skin flap for irradiation.

Mouse irradiation

A group of mice ($n=27$) were irradiated unidirectionally with MRT, with three adjacent fields, using different in-beam entrance doses (200 Gy, 400 Gy and 800 Gy). Another group of mice ($n=27$) were irradiated with three adjacent fields of BB radiation entrance doses of 200 Gy, 400 Gy and 800 Gy. A further set of mice were irradiated with BB radiation entrance doses of 11 Gy, 22 Gy and 44 Gy. The MRT and high dose BB array size was 6 mm × 6 mm. The low dose BB array size was 10 mm (horizontally) × 6 mm (vertically). The high dose BB and MRT dose rates were approximately 100 Gy s^{-1} and 80 Gy s^{-1}, respectively. We used six mice as sham-irradiated controls. These unirradiated mice were prepared, anaesthetised and positioned on the treatment jig in an identical fashion to the irradiated mice. Immediately post-irradiation, a fine gauge needle containing Evans blue dye (Sigma Aldrich, St Louis, MO) was used to mark the corners of the irradiated fields on the mice skin using the exposed radiochromic film as a visual guide. The overall irradiated region was marked with permanent marker. The mice recovered from the anaesthesia and were returned to the animal facility in the biomedical imaging centre at SPring-8.

Tissue harvesting

Mice were culled by cervical dislocation at specific time-points post-irradiation. There were 6 mice in each high dose category (MRT and BB) at each culling time, with the exception of the 6 h point, for which there were 3 mice in the MRT group and 3 in the BB group. In the low dose BB category (11 Gy, 22 Gy and 44 Gy), there were two mice at each culling time. Table 1 summarises the radiation doses and culling times of the mice. The skin flap was excised from the mouse, flattened and fixed in 10% neutral-buffered formalin for at least 6 h. Small sections of irradiated tissue, perpendicular to the path of the microbeams for each of the three delivered doses, were then removed and placed into histology cassettes. The tissue sections were returned to Australia in phosphate-buffered saline for analysis.

Table 1. Radiation doses and culling times post-irradiation

Modality	Peak entrance dose (Gy)	Valley dose (Gy)	Integrated dose (Gy)	Culling times post irradiation (h)
High dose BB (ddY mice)	200 400 800	N/A	200 400 800	6, 12, 24, 48 and 120
High dose MRT (ddY mice)	200 400 800	~2–4 ~4–8 ~8–16	~25 ~50 ~100	6, 12, 24, 48 and 120
Low dose BB (BALB/C mice)	11 22 44	N/A	11 22 44	4, 12, 24, 48 and 84
Control (ddY and BALB/C mice)	0	0	0	N/A

BB, broad-beam; MRT, microbeam radiotherapy.

Histology and immunohistochemistry

Haematoxylin and eosin

All tissue sections were embedded into paraffin wax blocks to enable sectioning on a microtome. A routine haematoxylin and eosin (H&E) staining protocol was used to stain the tissue sections. Both entrance and exit skin flaps were stained for histology; however, we performed our analysis only on the entrance fields. The section thickness for all histological and immunohistochemical sections was 5 μm.

γ-H2AX assay

The primary antibody was a 1:1000 dilution of anti-phosphohistone H2AX (Ser139) Clone JBW301 (Upstate, Temecula, CA) diluted in mouse-on-mouse (MOM) diluents (8:100 in tris-buffered saline). The MOM kit (also used for protein blocking) was purchased from Vector Labs Inc (Burlingame, CA) as BMK-2202. Antigen retrieval was carried out on the sections via microwave heating of citrate buffer (pH 6) for 10 min. The primary antibody was applied to the sections and allowed to sit overnight at 4°C. The MOM kit secondary antibody diluted in MOM diluent (1:250 in tris-buffered saline (TBS)) was applied to the sections for 10 min at room temperature. The primary antibody was detected using the Dako EnVision kit, as per the manufacturer's instructions (DAKO Corporation, Carpenteria, CA). Sections were stained using Harris's haematoxylin and 1% aqueous eosin.

A semi-quantitative assessment of acute radiation dermatitis was performed using H&E sections. The parameters used to analyse the radiation-induced damage were epidermal cell death identified by the presence of cells with ghosted outlines and lack of nuclear details (necrotic cells) or cells with dense cytoplasm and dark pyknotic nuclei (apoptotic bodies); adnexal damage defined as cell death or damage in the pilo-sebaceous units based on quantification of necrotic cells and apoptotic bodies in hair follicles or partial or complete absence of hair follicles and sebaceous glands; epidermal spongiosis (intercellular oedema); epidermal nuclear enlargement (variations in size of nucleus); and dermal inflammation. Each parameter was given a score of between 0–3 according to severity. Table 2 summarises the details of the scoring system used. Scoring was done using a high power (×40) objective lens with a field diameter of 0.5 mm and a surface area of 0.196 mm^2. The scorer was blind to the irradiation modality (high dose BB, MRT, low dose BB). The slides were numbered before scoring and the sequence was revealed after scoring. We compared and analysed the extent of skin damage following varying doses of MRT and BB at different time-points (Table 1). We also made qualitiative examinations of the distribution of apoptotic cells in the epidermis and hair matrix, in relation to irradiated strips

Table 2. Histological parameters used to quantify the skin changes. High power field (h.p.f) =0.196 mm^2

Parameter	Score 0	Score 1	Score 2	Score 3
Epidermal cell death	No apoptosis	1–5 apoptotic or necrotic bodies per 10 h.p.f.	⩾6 apoptotic or necrotic bodies per 10 h.p.f.	Full thickness epidermal necrosis
Spongiosis	No spongiosis	Focal	Involving lower 1/2 of the epidermis	Involving full thickness of the epidermis
Epidermal nuclear enlargement (average size 50 nuclei)	<10 μm	10–12 μm	12–15 μm	>15 μm
Adnexal damage	Normal hair follicles	1–5 apoptotic or necrotic bodies in pilo-sebaceous unit per 10 h.p.f.	⩾6 apoptotic or necrotic bodies in pilo-sebaceous unit per 10 h.p.f.	Partial loss of hair follicles
Dermal leukocytic infiltration	No leukocytic infiltration	Leukocytes covering <10% of the dermis	Leukocytes covering 10–70% of the dermis	Leukocytes covering >70% of the dermis

in MRT cases using sections co-stained with γ-H2AX and H&E.

Statistical analysis

We used the SPSS 17 statistical software program (SPSS Inc, Chicago, IL) to evaluate statistically significant differences in the histological parameters measured for different radiation modalities and times. Univariate ANOVA with *post hoc* correction was used to calculate *p*-values.

Results

The integrated epidermal cell death scores (averaged over 10 high power field (h.p.f)) in high dose MRT groups were significantly lower than the high dose BB groups at all time-points. The epidermal cell death scores in the 200 Gy and 400 Gy MRT groups were comparable to the low dose BB scores.

We observed apoptotic cells in the basal layer of the epidermis by 6 h post-irradiation in all cases of high dose MRT (200 Gy, 400 Gy and 800 Gy) and high dose BB (200 Gy, 400 Gy and 800 Gy). The epidermal cell death score gradually increased in the high dose BB groups, which may in part have lead to full-thickness epidermal necrosis by 120 h post-irradiation in all cases of 800 Gy and 400 Gy, and 1 case of 200 Gy BB (Figure 1a,d). Necrosis was not confined to the epithelial cells in the epidermis; we also observed ulceration extending to almost half the dermal depth in 4 mice in the 800 Gy BB group and 5 mice in the 400 Gy BB group by 5 days. The epidermal cell death scores in high dose MRT, were significantly lower than in the high dose BB groups ($p<0.0001$). We did not encounter full thickness epidermal necrosis in any case of high dose MRT at any time-point. Further, apoptotic score in the epidermis did not show any marked changes by 24, 48 or 120 h post irradiation in all three groups of high dose MRT. (Figure 1b,c). We observed a few scattered apoptotic cells (Score 1) in the epidermis in all three low dose BB groups (11, 22 and 44 Gy) across all time-points. There was no full thickness epidermal necrosis in the low dose BB groups. This finding is similar to that in 200 Gy and 400 Gy MRT. There were no significant differences in levels of epidermal cell death between low dose BB (all doses) and the 200 Gy and 400 Gy MRT dose groups ($p=0.904$). However, 800 Gy MRT caused significantly more epidermal cell death than 44 Gy BB by

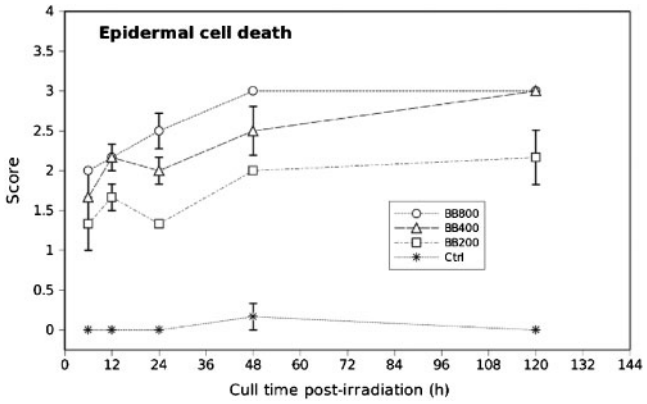

(a)

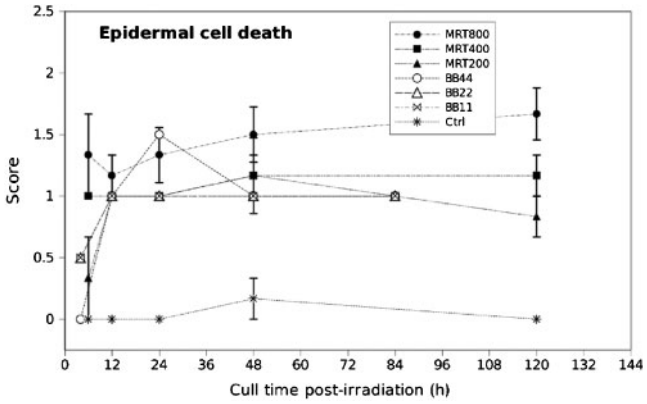

(b)

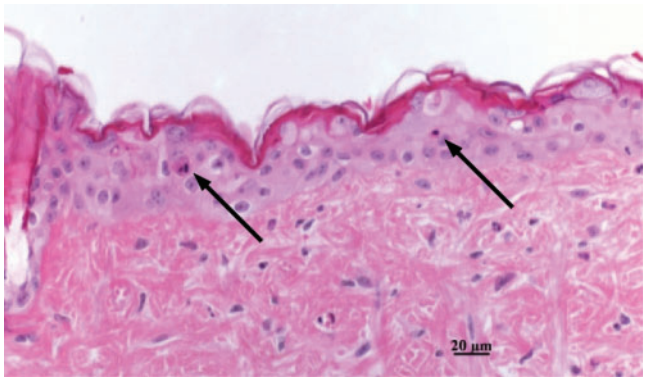

(c)

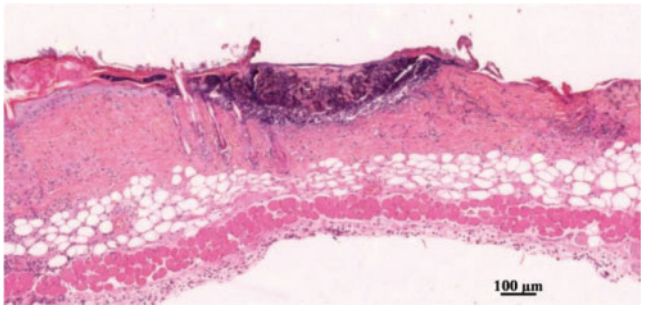

(d)

Figure 1. Epidermal cell death scores in (a) high dose broad-beam (BB) and (b) low dose BB and microbeam radiotherapy (MRT)-irradiated mouse skin tissue for different doses and times. (c) Score 1 (arrows show apoptosis) in 400 Gy MRT 5 days post-irradiation. (d) Score 3 (full thickness epidermal necrosis) in 400 Gy BB 5 days post-irradiation. Necrosis was not confined to the epithelial cells in the epidermis; we also observed ulceration extending to almost half the dermal depth in mice in the high dose BB group by day 5. The graphs in Figure 1 (and subsequent plots) contain connecting lines to aid visualisation only. The scoring data at the different time-points are from different mice. Error bars are standard error of the mean (SEM).

48 h ($p<0.0001$). We note the graphs in Figure 1 (and subsequent plots) contain connecting lines to aid visualisation only. The scoring data at the different time-points are from different mice.

The integrated adnexal damage scores (averaged over 10 h.p.f.) in the high dose MRT groups were significantly lower than the high dose BB groups at all time-points. The adnexal damage scores in the 200 Gy MRT group were comparable with the low dose BB groups (all doses).

We observed apoptotic cells in the hair follicles by 6 h post-irradiation in all cases of high dose MRT (200 Gy, 400 Gy and 800 Gy) and high dose BB (200 Gy, 400 Gy and 800 Gy). We did not observe partial or complete hair follicle loss in any case of high dose MRT at any time-point (based on quantification of necrotic and/or apoptotic bodies in hair follicles or partial or complete absence of hair follicles and sebaceous glands). The adnexal damage scores in the high dose MRT groups were significantly lower than the high dose BB groups at all time-points ($p<0.0001$). There were no significant differences in levels of adnexal damage between low dose BB (all doses) and the 200 Gy MRT dose group (Figure 2b). The apoptotic scores in the adnexa were lower 120 h post-irradiation than at 48 h post-irradiation in the high dose MRT cases (Figure 2b).

The occurrences of epidermal and adnexal cell death were not exclusively confined to the peak irradiated fields in MRT.

We qualitatively identified fields of irradiation with the use of γ-H2AX immunostaining, which showed positive cell nuclei in the peak irradiated fields. Although apoptotic bodies were mainly observed within the irradiated strips, there were also apoptotic bodies in epidermis and hair follicles in the non-irradiated areas (Figure 3a,b).

There was significantly more epidermal spongiosis in the high dose BB groups compared with the 200 Gy and 400 Gy MRT dose groups, but not compared with the 800 Gy MRT group. Epidermal spongiosis was undetectable in the low dose BB groups and the 200 Gy MRT group. In the 800 Gy groups, spongiosis or intercellular oedema first appeared by 24 h post-irradiation with both BB and MRT (Figure 4a). The spongiosis score gradually increased and reached a maximum at 48 h post-irradiation in 800 Gy BB (Figure 4), with 1 case showing intra-epidermal blister formation (Figure 4d). In the 800 Gy MRT group, there was a steady increase in spongiosis that peaked at 120 h and was comparable with the levels of spongiosis observed with high dose BB at the same time-point (Figure 4a,b). The 400 Gy MRT

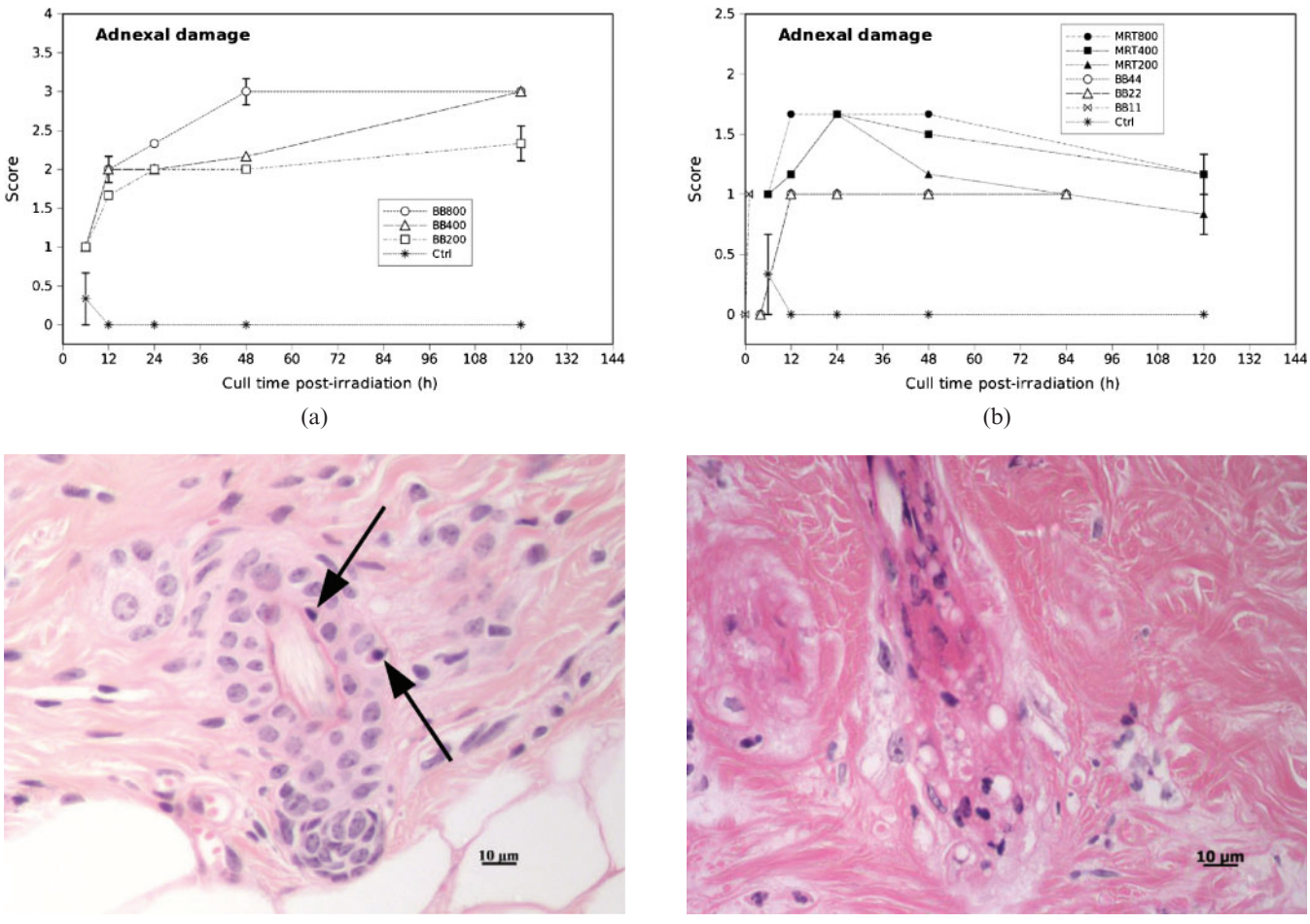

Figure 2. Adnexal damage scores in (a) high dose broad-beam (BB) and (b) low dose BB and MRT-irradiated mouse skin tissue for different doses and times. Error bars are standard error of the mean (SEM). (c) Score 1 (arrows show apoptosis). (d) Score 3 (partial loss of hair follicles).

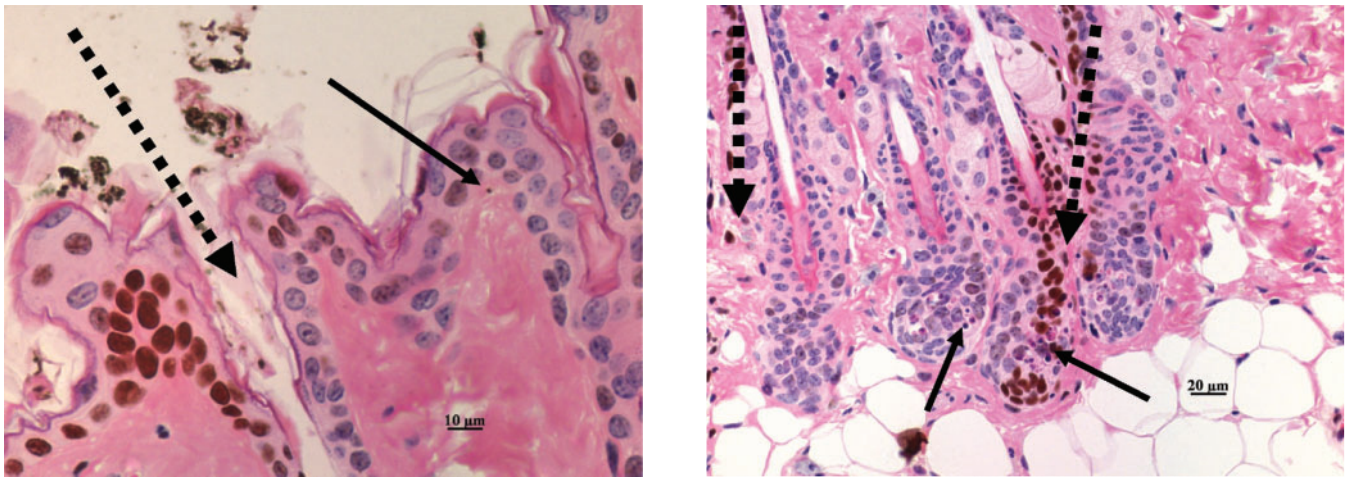

(a) (b)

Figure 3. Microbeam radiotherapy (MRT)-irradiated mouse skin stained with haematoxylin and eosin and the γ-H2AX immunohistochemical assay. (a) Apoptotic cell in "valley" region of epidermis; (b) apoptotic cell in both irradiated and non-irradiated hair follicles. Continuous arrows indicate apoptotic cells, dashed arrows indicate the path of the microbeams as inferred by γ-H2AX immunostaining.

group elicited some degree of epidermal spongiosis by 120 h post-irradiation but was not significantly different to the low dose BB groups and the 200 Gy MRT group (p=0.574). Spongiosis was undetectable in the low dose BB groups and the 200 Gy MRT group by 84 h and 120 h post-irradiation, respectively (Figure 4b).

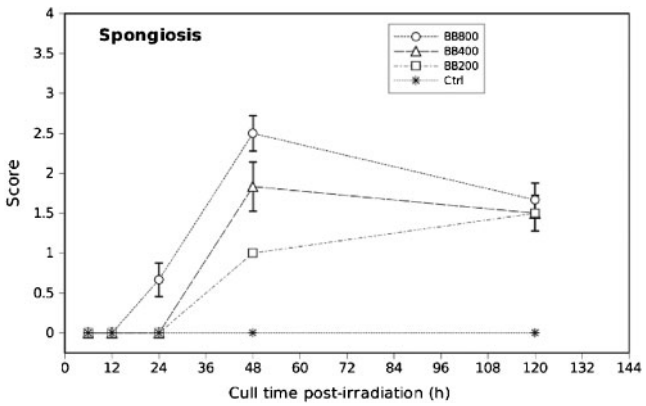

(a)

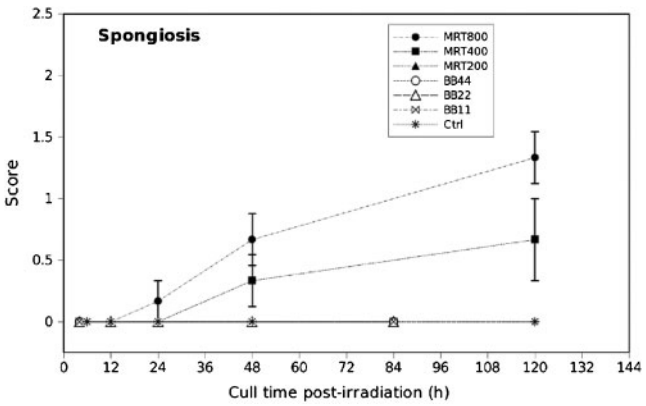

(b)

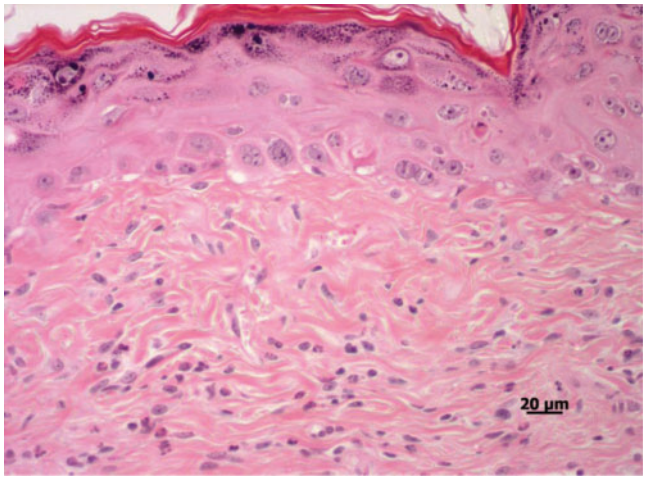

(c)

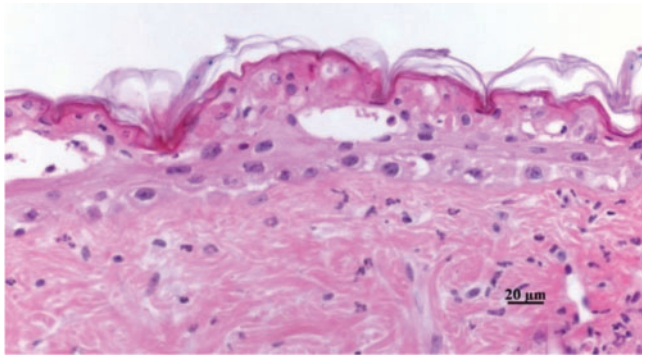

(d)

Figure 4. Epidermal spongiosis scores in (a) high dose broad-beam (BB) and (b) low dose BB and microbeam radiotherapy-irradiated mouse skin tissue for different doses and times. Error bars are standard error of the mean (SEM). (c) Spongiosis involving only the bottom third of the epidermis layer. (d) Spongiosis with intra-epidermal vesicles.

The epidermal nuclear enlargement score for 200 Gy and 400 Gy MRT was not significantly different than the low dose BB scores.

There were only a few cases of mild nuclear enlargement by 12 h post-irradiation, in both high dose BB (200 Gy, 400 Gy and 800 Gy) and MRT (200 Gy, 400 Gy and 800 Gy). High dose BB caused obvious nuclear enlargement by 48 h (Figure 5a). The extent of nuclear enlargement was maximum by 120 h with both high dose BB and MRT treatments (Figure 5a,b), most of which showed enlarged epidermal keratinocytes with scattered giant nuclei measuring up to 18 μm in cross-sectional diameter, with irregular nuclear membranes and multiple nucleoli (Figure 5d). All three dose groups of high dose BB showed greater nuclear enlargement in epidermal cells than with high dose MRT. None of the low dose BB cases showed epidermal nuclear enlargement by 84 h post-irradiation. The nuclear enlargement score for 800 Gy MRT was inbetween the high dose BB and the low dose BB scores. There was no statistically significant difference in nuclear enlargement score for 400 Gy MRT and 22 Gy BB (p=0.322) and for 200 Gy MRT and 11 Gy BB (p=0.486) (Figure 5b).

Dermal leukocytic infiltration was higher in high dose BB than high dose MRT (Figure 6). The 400 Gy and 200 Gy MRT groups did not have significantly different leukocyte scores than the 22 Gy and 11 Gy BB groups.

We observed dermal neutrophils (leukocytes) by 6 h post irradiation in all cases of high dose BB (200 Gy, 400 Gy and 800 Gy), whereas leukocytes first appeared 12 h post irradiation in high dose MRT (Figure 6a–c). The density of the leukocytic infiltrate peaked 24 h post-irradiation in 800 Gy BB and persisted at the same level until 120 h (Figure 6a). Infiltration was maximal by 120 h in the 200 and 400 Gy BB groups. After 48 h there were a few lymphocytes mixed with neutrophils; however, neutrophils were the predominant inflammatory cell component throughout the study. The inflammatory cells were more obvious at the deep dermis and in most cases extended to the subcutaneous tissue (Figure 6d). In high dose MRT groups, leukocytic infiltration decreased towards 120 h post irradiation (Figures 6b–c). Two cases of 200 Gy MRT did not show leukocytic cells by 120 h. Low dose BB cases (11, 22 and 44 Gy) showed very mild dermal leukocytic infiltration throughout the study period. There was no statistically significant difference in dermal leukocytic infiltration between 400 Gy MRT and 22 Gy BB at the 0.05 level (p=0.113) and there was borderline statistical significance in infiltration between 11 Gy BB and 200 Gy MRT (p=0.075). There was a statistically significant

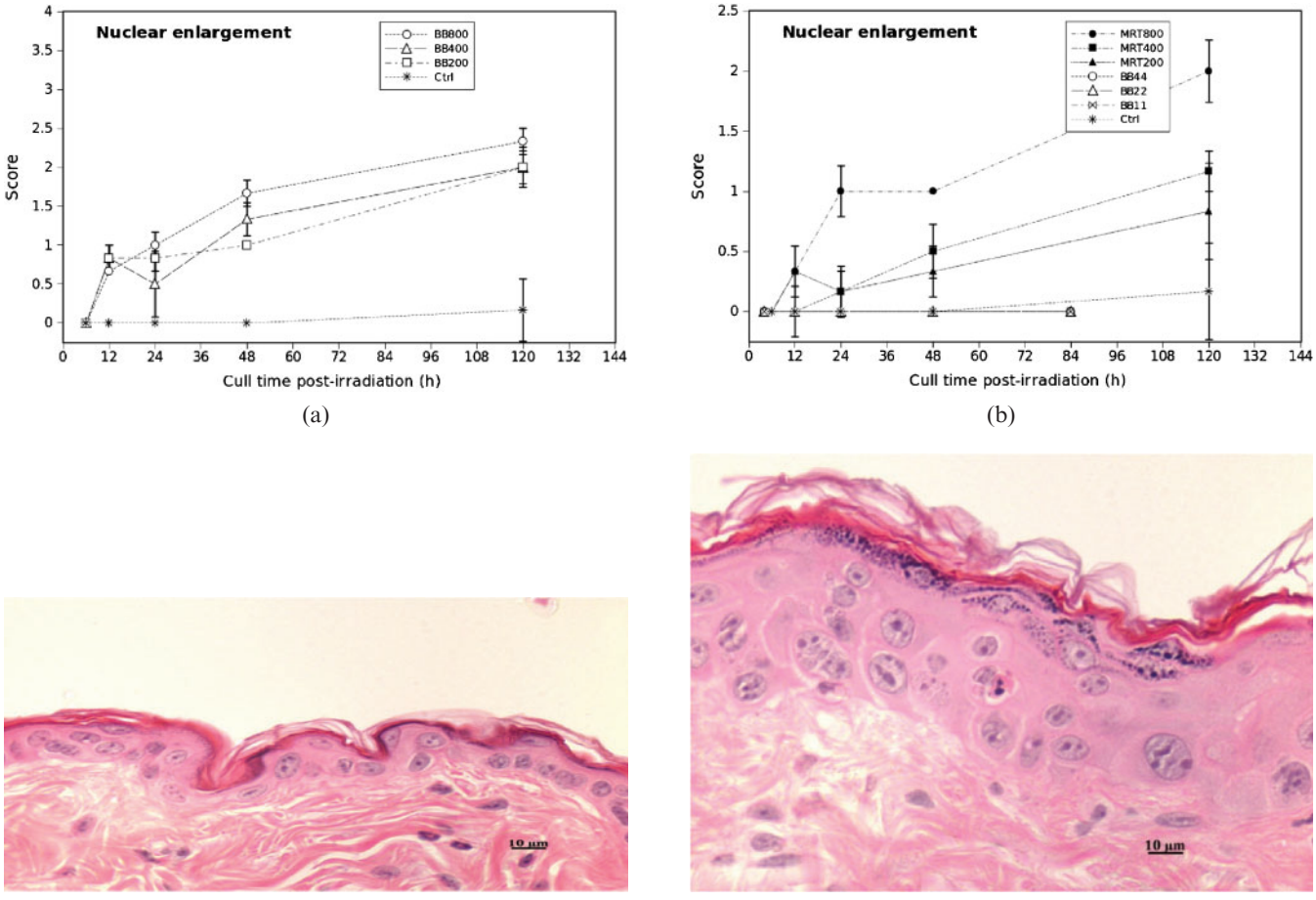

Figure 5. Epidermal cell nuclear enlargement scores in (a) high dose broad-beam (BB) and (b) low dose BB and microbeam radiotherapy (MRT)-irradiated mouse skin tissue for different doses and times. Error bars are standard error of the mean (SEM). (c) Score 1; (d) Score 3.

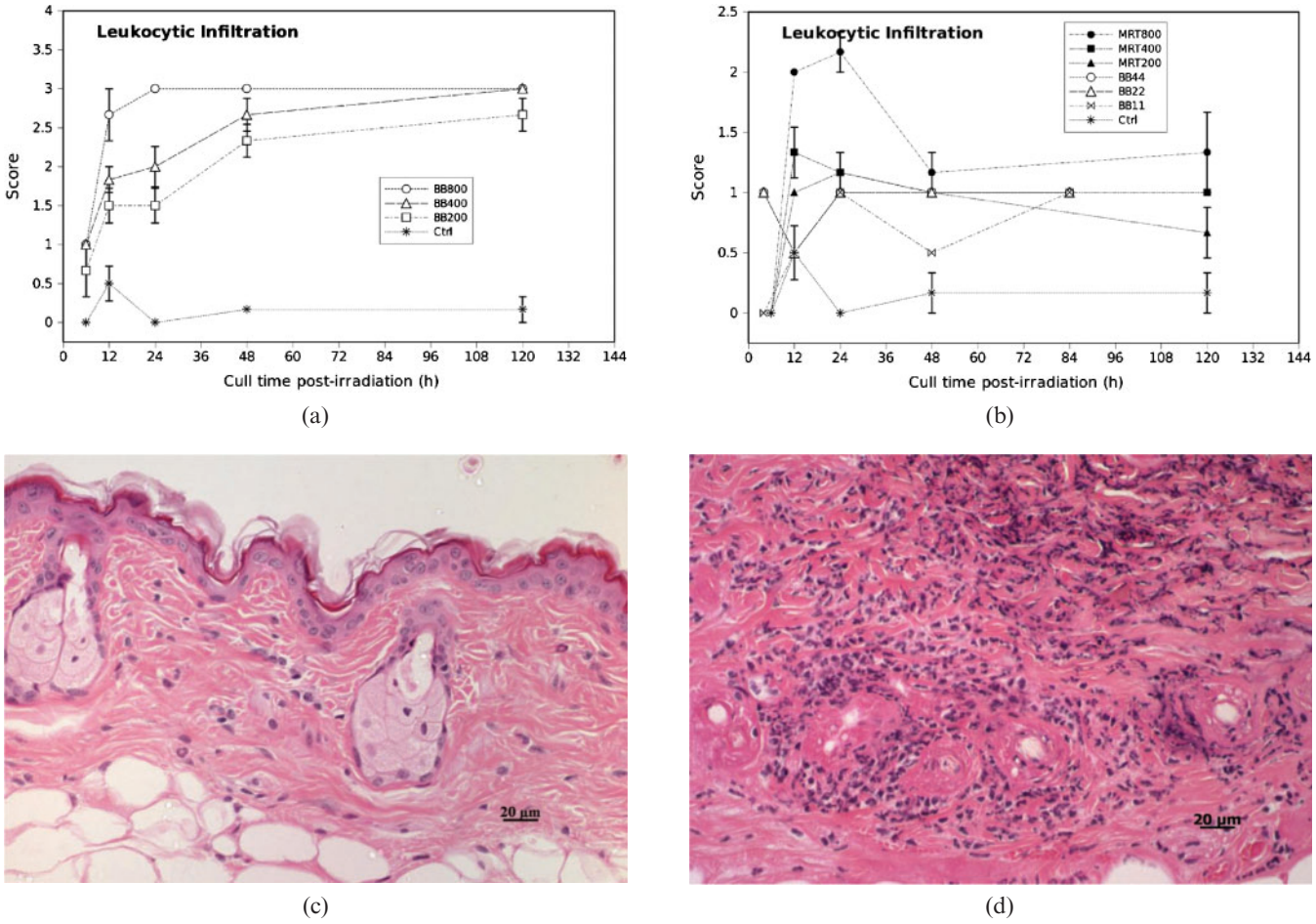

Figure 6. Leukocytic infiltration scores in (a) high dose broad-beam (BB) and (b) low dose BB and microbeam radiotherapy (MRT)-irradiated mouse skin tissue for different doses and times. Error bars are standard error of the mean (SEM). (c) Occasional neutrophils covering <10% of the dermis (Score 1). (d) Dense infiltrate of neutrophils covering >70% of the dermis (Score 3).

difference in the extent of dermal leukocytic infiltration between 800 Gy MRT and 44 Gy BB ($p<0.0001$).

Discussion

Our most important finding is that peak entrance doses of 200 Gy and 400 Gy MRT produced a similar pathological response to low dose BB (11, 22 and 44 Gy). In this study we quantified the acute effects of high dose MRT, high dose BB and low dose BB in normal mouse skin using a dermatopathological scoring system. The use of such a scoring system allows us to compare BB with MRT from a purely biological perspective with less emphasis on the physical dosimetry. Table 3 summarises our principal findings for MRT and low dose BB.

In this study we showed that the extent of epidermal cell death, hair follicle damage, epidermal spongiosis, nuclear enlargement and dermal leukocytic infiltration in high dose BB was greater than that for high dose MRT. This finding is perhaps not surprising given the smaller integrated dose of MRT compared with BB at equivalent peak entrance doses (Table 1).

The integrated MRT doses, defined as the peak dose multiplied by the ratio of the beam width to beam spacing (about 12.5% in our study), for 200 Gy MRT

Table 3. Summary of principal findings for microbeam radiotherapy (MRT) and low dose broad-beam (BB)

Pathological parameter	Comparison
Epidermal cell death	400 Gy, 200 Gy MRT not significantly different to low dose BB (44, 22 and 11 Gy)
Adnexal damage	200 Gy MRT not significantly different to low dose BB (all doses)
Spongiosis	400 Gy and 200 Gy MRT not significantly different to 22 Gy and 11 Gy BB
Nuclear enlargement	400 Gy, 200 Gy MRT not significantly different to low dose BB (44, 22 and 11 Gy)
Dermal leukocytic infiltration	800 Gy MRT significantly different to 44 Gy BB, 400 Gy MRT not significantly different to 22 Gy BB, 200 Gy MRT borderline differences compared with 11 Gy BB

(integrated dose approximately 25 Gy) and 400 Gy MRT (integrated dose approximately 50 Gy) were comparable with the 22 Gy and 44 Gy doses in our low dose BB group (Tables 1 and 3). This finding is important because it indicates that the integrated dose in MRT may be more relevant than the peak or valley dose in determining the acute pathological response of radiation dermatitis, at least in mouse skin tissue. The valley dose, as seen in Table 1, was only 1–2% of the peak dose [10].

Double staining sections with γ-H2AX/H&E (Figure 3) showed that epithelial cell apoptosis, spongiosis and leukocytic infiltration were not confined to the path of the microbeams through the tissue. This is not entirely surprising for biological processes such as spongiosis and inflammation where intracellular signalling and leukocyte migration are likely to occur some distance from radiation damaged cells. It is also possible that some cells may have migrated out from the irradiated zones and subsequently become apoptotic. In support of this concept, we have previously reported migration of tumour cells post-synchrotron MRT [25]. The absorbed dose in the valley region was estimated to be between 2 and 16 Gy depending on the peak dose (Table 1). These valley doses may have been high enough to explain pathological damage outside the peak regions. An alternative explanation for damage outside of the irradiated zones is local radiation-induced cellular communication (a type of bystander effect) due to release of cytokines and other factors from damaged cells. However, we do not have any direct evidence to confirm such a hypothesis, as yet.

Despite physical dosimetry differences, there were some similar histological observations in our present study and the study by Zhong et al [7] on MRT to rat skin. Zhong et al reported hypertrophy of the epidermis and damage to hair follicle structure 3–6 days post 900 Gy MRT and necrotic/pyknotic cells appeared in the matrix (of the follicle). They observed no epidermal denudation or exudation 6 days post 900 Gy MRT. These findings are similar to our own; however, they noted that the sebaceous glands had disappeared by day 6 post 900 Gy MRT, something we did not. The disappearing sebaceous glands in Zhong et al's study may be a result of their higher integrated dose. For example, for a skin entrance in-beam dose of 835 Gy, their valley dose was approximately 21 Gy and their integrated dose approximately 260 Gy, based on Monte-Carlo simulations (Table 1 in [7]).

John Hopewell described the special cases of acute ulceration and acute epidermal necrosis in his review of the skin's response to ionising radiation [14]; the former being "an early loss (<14 days) of the epidermis and to a varying degree, deeper dermal tissues as a result of the death of cells in interphase", and the latter as "(<10 days) interphase death of post-mitotic keratinocytes in the upper viable layers of the epidermis". These cases are associated with high doses of radiation and are phenomena we observed in our high dose BB groups, in particular 400 Gy and 800 Gy BB, 5 days post-irradiation (Figure 1e).

Our findings are limited in scope to the first 5 days post-irradiation. Subacute and chronic changes weeks and months post-irradiation are also important to understand the dermatopathology of radiation dermatitis. With data at longer time-points, we could make further comparisons with Zhong et al [7] and with, for example, some of Hopewell's rodent skin experiments using small field sizes [24].

As noted in our Introduction and elsewhere [25], measurement-based dosimetry is challenging owing to the different components of the MRT dose profile. The pathological scoring approach described in this study is concerned with the tissue's radiobiological response, irrespective of modality. Biological methods of dosimetry may play an important role in MRT as a way of predicting the normal tissue toxicity and comparing it with conventional RT. This might have useful applications for future clinical (*i.e.* human) trials of MRT.

Conclusion

We report the extent of skin damage in high dose MRT was significantly lower than for high dose BB, but more importantly, high dose MRT elicited a similar pathological response as low dose BB. The integrated MRT dose was a more useful dosimetric parameter for comparing the response of mouse skin with BB radiation fields than either the peak or valley doses. The damage from MRT (particularly spongiosis and leukocytic infiltration) was spread evenly across the skin tissue and not exclusively confined to regions or zones of high dose.

Acknowledgments

RCUP received financial support from the Victorian Cancer Biobank. Our synchrotron MRT research was supported by funding from the Cancer Council Victoria Venture Grant scheme, the Access to Major Research Facilities Program, administered by the Australian Nuclear Science and Technology Organisation, and Monash University. PAWR received a National Health and Medical Research Council of Australia Fellowship (Grant No. 143805). We thank Leonie Cann from the Centre for Women's Health Research, Monash University for assisting with experimental work and preparing histological stains of the tissue sections. We thank our colleagues at the SPring-8 synchrotron in Japan, particularly Dr Naoto Yagi.

References

1. Dilmanian FA, Button TM, Le Duc G, Zhong N, Pena LA, Smith JA, et al. Response of rat intracranial 9L gliosarcoma to microbeam radiation therapy. Neuro-oncol 2002;4:26–38.
2. Dilmanian FA, Morris GM, Zhong N, Bacarian T, Hainfeld JF, Kalef-Ezra J, et al. Murine EMT-6 carcinoma: high therapeutic efficacy of microbeam radiation therapy. Radiat Res 2003;159:632–41.
3. Laissue JA, Geiser G, Spanne PO, Dilmanian FA, Gebbers JO, Geiser M, et al. Neuropathology of ablation of rat gliosarcomas and contiguous brain tissues using a microplanar beam of synchrotron-wiggler-generated X rays. Int J Cancer 1998;78:654–60.
4. Miura M, Blattmann H, Brauer-Krisch E, Bravin A, Hanson AL, Nawrocky MM, et al. Radiosurgical palliation of aggressive murine SCCVII squamous cell carcinomas using

synchrotron-generated X-ray microbeams. Br J Radiol 2006;79:71–5.
5. Serduc R, Bouchet A, Brauer-Krisch E, Laissue JA, Spiga J, Sarun S, et al. Synchrotron microbeam radiation therapy for rat brain tumor palliation-influence of the microbeam width at constant valley dose. Phys Med Biol 2009;54:6711–24.
6. Smilowitz HM, Blattmann H, Brauer-Krisch E, Bravin A, Di Michiel M, Gebbers JO, et al. Synergy of gene-mediated immunoprophylaxis and microbeam radiation therapy for advanced intracerebral rat 9L gliosarcomas. J Neurooncol 2006;78:135–43.
7. Zhong N, Morris GM, Bacarian T, Rosen EM, Dilmanian FA. Response of rat skin to high-dose unidirectional x-ray microbeams: a histological study. Radiat Res 2003;160: 133–42.
8. Brauer-Krisch E, Serduc R, Siegbahn EA, Le Duc G, Prezado Y, Bravin A, et al. Effects of pulsed, spatially fractionated, microscopic synchrotron X-ray beams on normal and tumoral brain tissue. Mutat Res 2010;704:160–6.
9. Brauer-Krisch E, Bravin A, Lerch M, Rosenfeld A, Stepanek J, Di Michiel M, et al. MOSFET dosimetry for microbeam radiation therapy at the European Synchrotron Radiation Facility. Med Phys 2003;30:583–9.
10. Crosbie JC, Svalbe I, Midgley SM, Yagi N, Rogers PA, Lewis RA. A method of dosimetry for synchrotron microbeam radiation therapy using radiochromic films of different sensitivity. Phys Med Biol 2008;53:6861–77.
11. Nettelbeck H, Takacs GJ, Lerch ML, Rosenfeld AB. Microbeam radiation therapy: a Monte Carlo study of the influence of the source, multislit collimator, and beam divergence on microbeams. Med Phys 2009;36:447–56.
12. Siegbahn EA, Stepanek J, Brauer-Krisch E, Bravin A. Determination of dosimetrical quantities used in microbeam radiation therapy (MRT) with Monte Carlo simulations. Med Phys 2006;33:3248–59.
13. Dilmanian FA, Kalef-Ezra J, Petersen MJ, Bozios G, Vosswinkel J, Giron F, et al. Could X-ray microbeams inhibit angioplasty-induced restenosis in the rat carotid artery? Cardiovasc Radiat Med 2003;4:139–45.
14. Hopewell JW. The skin: its structure and response to ionizing radiation. Int J Radiat Biol 1990;57:751–73.
15. Malkinson FD, Keane JT. Radiobiology of the skin: review of some effects on epidermis and hair. J Invest Dermatol 1981;77:133–8.
16. Cornelison RL, Crowson AN. Cutaneous reactions to exogenous agents. In: Barnhill R, editor. Dermatopathology. 3rd edn. McGraw-Hill Professional; 2010.
17. Fajardo LF. Morphology of radiation effects on normal tissues. In: Perez CA, Brady LW, editors. Principles and Practice of Radiation Oncology. 2nd edn. J.P. Lippincott Company; 1992.
18. Hall EJ. Dose response relationships for model normal tissues. In: Radiobiology for the Radiologist. 5th edn: Lippincott Williams & Wilkins; 2000.
19. van Der Kogel A. Radiation response and tolerance of normal tissues. In: Steel GG, editor. Basic Clinical Radiobiology. 3rd edn: Arnold; 2002.
20. McKee PH, Calonje E, Granter SR. Diseases of collagen and elastic tissue. In: Pathology of the skin: with clinical correlations 3rd edn: Elsevier Mosby; 2005: 1055–8.
21. Lever WF, Schaumburg-Lever G. Inflammatory diseases due to physical agents and foreign substances. In: Histopathology of the skin. 7th edn: JB Lippincott Company; 1990: 235–7.
22. Straile WE, Chase HB. The use of elongate microbeams of X-rays for simulating the effets of cosmic rays on tissues: A study of wound healing and follicle regeneration. Radiat Res 1963;18:65–75.
23. Ohno Y, Torikoshi M, Suzuki M. Dose distribution of a 125 keV mean energy microplanar x-ray beam for basic studies on microbeam radiotherapy. Med Phys 2008;35:3252–8.
24. Hopewell JW, Coggle JE, Wells J, Hamlet R, Williams JP, Charles MW. The acute effects of different energy beta-emitters on pig and mouse skin. Br J Radiol Suppl 1986;19:47–51.
25. Crosbie JC, Anderson RL, Rothkamm K, Restall CM, Cann L, Ruwanpura S, et al. Tumor cell response to synchrotron microbeam radiation therapy differs markedly from cells in normal tissues. Int J Radiat Oncol Biol Phys 2010;77:886–94.